ORIGINAL ARTICLE

Bedload transport and bedforms migration under sand supply limitation

Mélanie Vah[1] · Armelle Jarno[1] · Sophie Le Bot[2] · Yann Ferret[2,3] · François Marin[1]

Abstract

Most studies on sediment transport and bedforms migration consider unlimited sediment supply conditions. However, areas where the sediment supply is limited are common in coastal and fluvial environments. The present paper, based on physical modelling in a flume and on a re-analysis of field data obtained in the Eastern English Channel by Ferret (Morphodynamique des dunes sous-marines en contexte de plate-forme mégatidale (manche orientale). approche multi-échelles spatio-temporelles, 2011), considers the effects of sediment supply limitation on bedload transport and bedforms migration velocity. The bedload transport is found to be proportional to the fraction of the bed covered by sediments for a bed exhibiting bedforms. The migration velocity of bedforms depends on the dominant mode of sediment transport. A new formulation showing a good agreement with experimental tests and observations in the field is proposed for the dimensionless migration velocity of these bedforms when sediment transport is dominated by bedload, under unlimited sediment supply conditions. For limited sediment supply conditions and sediment transport dominated by bedload, an adaptation of the formulation is suggested from flume data sets, based on the fraction of the bed covered by sediment.

✉ François Marin
   francois.marin@univ-lehavre.fr

   Mélanie Vah
   melanie.vah@univ-lehavre.fr

   Armelle Jarno
   jarnoa@univ-lehavre.fr

   Sophie Le Bot
   sophie.lebot@univ-rouen.fr

   Yann Ferret
   yann.ferret@shom.fr

[1] UNIHAVRE, CNRS, LOMC, Normandie Univ, 76600 Le Havre, France

[2] UNIROUEN, UNICAEN, CNRS, Normandie Univ, M2C, 76000 Rouen, France

[3] Present Address: SHOM, 13, rue du Chatellier, CS 92803, 29228 Brest Cedex 2, France

1 Introduction

Sediment supply limitation can significantly impact sediment transport and bedforms. This topic has received little attention when compared to the extended literature dedicated to unlimited sediment-supply conditions in coastal and fluvial environmental contexts, even if in situ conditions where the mobile sediment stock is limited are not so uncommon (Engelund and Fredsøe [21], Blondeaux [7], van Landeghem et al. [50], Seminara [42], Colombini and Stocchino [16], Charru et al. [13] among others). Sediment limitation can be due to a small sediment supply on an unerodible bottom or partially mobile sediment bed (case of strong sediment heterogeneity). For example, Carling et al. [10, 11] described large sandy barchans (crescent-shaped dunes) migrating over an armoured layer in the Rhine (Germany). In the coastal context of the English Channel, the sediment layer is highly heterogeneous with a mixture of grains of various sizes and shapes, leading sometimes to a significant sediment gradient between immobile zones and regions rich in movable sediments (Le Bot and Trentesaux [33], Ferret et al. [24]).

Studies under unlimited amount of sediments are common in the literature to describe bedform dimensions but also for sediment transport and bedform migration. The characterization of mature bedforms such as ripples or dunes has lead to a lot of studies. Ripples are often considered to scale with the grain size while dunes scale with the water depth (Kennedy [30]; Flemming [25]). Generally, no dependence on the bottom shear-stress conditions is involved in the formulations for ripple dimensions (Allen [1], Soulsby et al. [45] among others). In situ measurements of bedload transport is a challenge (for example Ribberink [41], Durafour et al. [20]) and most of the time bedload transport is estimated. Prediction of sediment transport and more specifically bedload transport was also extensively studied (Meyer-Peter and Müller [35], Fernandez Luque and Van Beek [22], Nielsen [36], Ribberink [41] among others) with formulations based on the shear stress on flat bottom.

Bedload transport controls bedform migration. Franklin and Charru [28] and Florez and Franklin [26] proposed a model for bedforms migration velocity based on Meyer-Peter and Müller [35] bedload transport law. In situ migration measurements on short periods (few hours) with a high precision are difficult to obtain, especially for small bedforms such as ripples. However some studies where performed using video system or multi-beam echosounder. Nevertheless results from these studies were not used or compared with bedform migration model. Durafour [19] estimated the migration velocity of a ripple with a video system settled on the bottom during a tide. Doré [17] measured the migration velocity of a dune and superimposed ripples several times during a tide in the bay of Arcachon (France) with an echosounder. Both of these in situ measurements were obtained on infinite well-sorted sediment supply and in a tidal flow context. Claude et al. [14] and Wintenberger et al. [54] carried out such measurements, using a multi-beam echosounder, in the Loire river for dunes with heterogeneous sediments in non limited supply conditions. Ferret et al. [24] measured the migration of large dunes, in the Eastern English Channel, also using a multi-beam echosounder, for various sediment supply conditions, on long periods (annual to pluri-decadal) but also on short periods (flood or ebb phases to several days).

Bedforms under sediment supply limitation have been experimentally studied in fluvial conditions at the equilibrium state by Tuijnder et al. [48], Tuijnder [46], and Dréano et al. [18]. Tuijnder et al. [48] found that the equilibrium dune dimensions depend on the initial sediment thickness and on the dune height at the equilibrium state under unlimited supply conditions. Belderson et al. [5] noticed from field observations that different bedforms types are observed depending on sediment supply and current velocity. Kleinhans

et al. [31] worked on the occurrence of bedforms in sediment supply-limited conditions from experiments in flume and field observations (river Allier, France and river Waal, The Netherlands) and found that bedform shapes depend on the supply limitation. Rauen et al. [40] used a divergent flume to study the supply limitation impact coupled to non-uniform flow and found that the supply limitation mostly impact the steady state dimensions of bedforms. Porcile and Blondeaux [39] carried out theoretical studies on the initiation of bedforms for strong sediment supply limitation and tidal flow, using a linear instability approach. A good agreement was found with in situ data from Le Bot and Trentesaux [33]. Experimental and numerical works under oscillatory flow with very limited amount of sediment were performed by Blondeaux et al. [8] and Mazzuoli et al. [34], respectively and show that the wavelengths are longer in very supply limitation than under unlimited supply.

Tuijnder and Ribberink [47] proposed an experimental law to describe bedload transport under supply limitation based on flume tests carried out in fluvial conditions with varied slopes. They found a dependency of the bedload transport with the fraction of the bed covered by mobile sediment. Preliminary flume experiments with an unidirectional flow and without bottom slope have been conducted by Vah et al. [49]. No formulation for bedload transport under supply limitation in a coastal context already exists to the authors knowledge.

The present study focuses on bedload sediment transport and bedform migration under sand supply limitation, and extends the work of Tuijnder and Ribberink [47] and Tuijnder [46]. Tests are performed in a flume with a horizontal bottom at this aim, and the field data obtained in the Eastern English Channel by Ferret [23] are re-analysed.

2 Experimental setup and tests conditions

Experiments were carried out in a current flume. This flume is 10-m-long, 0.49-m-wide, and without slope (Fig. 1). The current is generated by a recirculating pump. The flow rate is measured with an ultrasonic flowmeter (Ultraflux) and can be adjusted in the range 0–100 L/s. The mean water depth d is measured above the initially flat bed at the beginning of each test. To ensure uniformity of the flow, a honeycomb was installed at
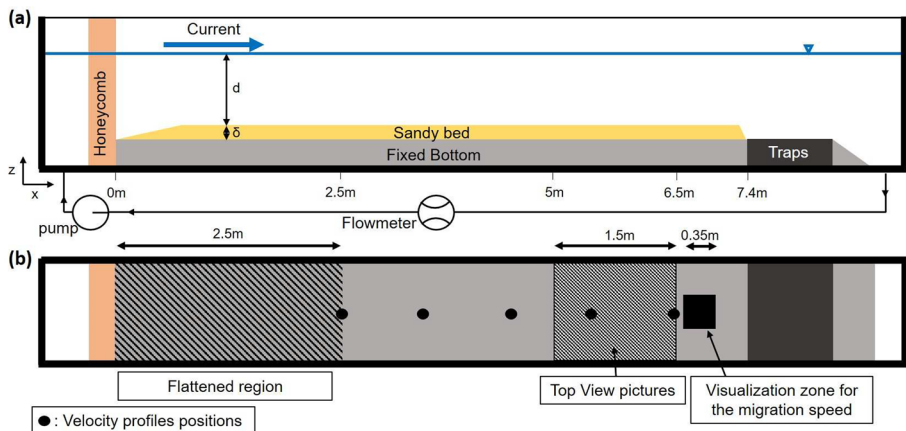
Fig. 1 Current flume with the different experimental zones. **a** Side view, **b** top view

the entrance of the flume. The distance between the honeycomb in the upstream part of the flume and the traps for the bedload sediment transport measurements is 7.4 m (Fig. 1). The bottom of the flume is made of polyvinyl chloride (PVC). A hand sanding machine equipped with a coarse sand abrasive disk is used to adjust the roughness level to a homogeneous micro-surface roughness. The resulting roughness can be estimated to a few micrometers which corresponds to a smooth hydraulic bottom.

For present tests, two different types of natural sand were selected. These sands are composed of quartz of relative density $s = \rho_s/\rho = 2.65$ where ρ_s and ρ are the sand and fluid density in clear water, respectively, and come from a quarry. According to Wentworth [52] classification, one of the two sands is of medium grain size ($250\,\mu m < D_{50} < 500\,\mu m$) with a median diameter $D_{50} = 328\,\mu m$ and the second sand is a coarse sand ($500\,\mu m < D_{50} < 1000\,\mu m$) with $D_{50} = 617\,\mu m$. Both sands are well-sorted according to Soulsby [44] criterion, with the geometric standard deviation defined by $\sigma_g^2 = D_{84}/D_{16}$ equal to 1.5 and 1.4 respectively, where D_{84} and D_{16} are the grain sizes respectively exceeded by 84% and 16% by weight of a sample of sediment.

All tests are conducted according to the same experimental protocol. First, the sand bed is flattened to reach a thickness noted δ (Fig. 1). The current is then generated in the flume, with a constant acceleration. The flow is ramped monotonically for approximately 1.5 min to reach the desired flow value. A similar ramp-down is applied to stop the flow when data acquisition of the bed topography is planned or traps need to be emptied. During the tests, stops were executed after 15 min to 1 h according to the current velocity, till a steady state for the bedload transport and the bedforms morphology is reached. At each stop the sediments found in the downstream traps are collected and spread evenly in the upstream flattened region of the flume ($0\,m < x < 2.5\,m$ where x is the distance from the honeycomb measured in the horizontal direction; Fig. 1b). This sediment transfer fulfills the quasi-constant sediment supply condition (Berni et al. [6]). Sediments are collected in each trap and weighted (Fig. 2). The lateral traps LT are used to quantify edge effects. These effects lead to a reduction of the sediment transport in the lateral traps LT compared to the central traps T1, T2, T3 (Fig. 2). A 20% maximum reduction is obtained for Set C2 (Table 1), when a 10% reduction is found for Sets M1, M2 and C1 (Table 1). No reduction is obtained for Sets M3 and C3 (Table 1). The percentage of sediment in traps T2, T3 and the final trap FT is negligible for tests with the coarse sediment and remains lower than 8% for the other tests compared to the quantity of sediment in traps T1.

After each current restart and when the steady current is reached, a video sequence of 450 s of the downstream part of the sandy zone is recorded (see Fig. 1). Then a series of images is extracted with a frequency of 1 Hz which is enough to capture the displacement of the structures. The same horizontal line of length 35 cm directed along the flume is selected in the stack of images and these lines are compiled to construct a spatio-temporal image (spatial resolution: 0.5 mm per pixel).

Fig. 2 Schematic view of the downstream traps. The arrow represents the flow direction
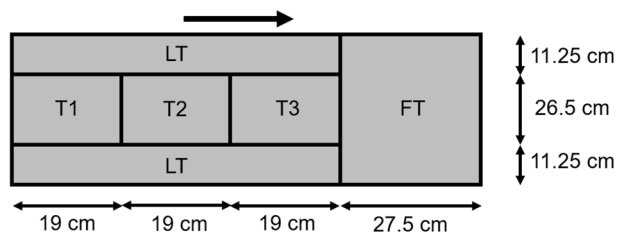
Table 1 Test conditions

	Set M1	Set M2	Set M3	Set C1	Set C2	Set C3
D_{50} (µm)	328	328	328	617	617	617
d (m)	0.25	0.25	0.25	0.195	0.25	0.25
U (m/s)	0.35	0.45	0.55	0.45	0.45	0.55
u'_* (m/s)	0.016	0.021	0.026	0.024	0.023	0.029
R (m)	0.124	0.124	0.124	0.109	0.124	0.124
W_s (m/s)	0.049	0.049	0.049	0.087	0.087	0.087
k_s (µm) (Nielsen [37])	820	820	820	1543	1543	1543
δ values (cm)						
0.1	x	x		x	x	
0.5	x	x	x	x	x	x
1	x	x	x	x	x	x
2	x	x	x	x	x	x
3.5	x (US)	x (US)	x	x	x	x
5.5	x (US)	x (US)	x (US)	x (US)	x (US)	x (US)
Type of bedforms at the equilibrium state (US conditions)	Ripples	Ripples	–	Dunes	Dunes	Dunes
Re	87,500	112,500	137,500	87,500	112,500	137,500
θ'	0.050	0.084	0.127	0.059	0.055	0.084
θ_c	0.036	0.036	0.036	0.030	0.030	0.030
D_*	8.3	8.3	8.3	15.6	15.6	15.6
R_{ep}	23.9	23.9	23.9	61.7	61.7	61.7
Re_*	13.1	17.2	21.3	37.0	35.5	44.7
b	10	7.5	5.6	8.6	9.3	6.5

Dimensional and dimensionless parameters

M medium sand, *C* coarse sand, *US* unlimited supply

Top view pictures of a 1.50 m long extended region (5 m < *x* < 6.5 m; Fig. 1) are regularly taken with a high resolution camera (0.1 mm per pixel) to obtain the wavelength of bedforms and the covered bed fraction.

The conditions of the test sets are given in Table 1, where δ is the initial thickness of sand on the bed. Sets M1, M2 and M3 are performed with the medium sand whereas sets C1, C2 and C3 are carried out with the coarse one. For each test set, 6 different tests are performed with different sediment supply conditions (except for sets M3 and C3 for which 5 supply conditions are considered).

The main dimensionless parameters involved in this study are the Reynolds number (Re), the Shields parameter (θ), and the Rouse number (b).

The flow Reynolds number and the effective Shields parameter are defined as follows:

$$Re = \frac{Ud}{\nu} \tag{1}$$

$$\theta' = \frac{u'^2_*}{(s-1)gD_{50}} \tag{2}$$

where U is the mean flow velocity, v the fluid kinematic viscosity, u'_* the effective shear velocity at bed based on the grain size, and g the acceleration due to gravity.

Measurements of the horizontal component of velocity u have been performed without sediment as preliminary tests with a laboratory Acoustic Doppler Current Profiler (ADCP Ubertone 1.5 MHz—step measurement: 0.375 mm—blank below free surface: 2 cm) (Fig. 3). The results show established velocity profiles from 3.5 m downstream of the honeycomb. The flow regime was turbulent for all the tests since the value of the Reynolds number was greater than 5000, the critical value for the flow to be turbulent (Sleath [43]; Table 1).

Figure 3 depicts the variation of u with z, the distance from the bed in the vertical direction, for different values of the mean flow velocity at $x = 6.5$ m. This figure exhibits logarithmic velocity profiles, approximately for $0.04 < z < 0.1$ m, characteristic of a turbulent flow. In the logarithmic layer, the velocity distribution may be written (Sleath [43]):

$$\frac{u(z)}{u'_*} = \frac{1}{\kappa} ln\left(\frac{z}{z_0}\right) \tag{3}$$

where z_0 is a length scale and $\kappa = 0.4$ the von Karman constant.

For present tests with sand, the values of the roughness Reynolds number $Re_* = u'_* k_s / v$ are in the range 13.1–44.7 (Table 1), where $k_s = 2.5 D_{50}$ (Nielsen [37]) is the roughness length of the bed. We have $5 < Re_* < 70$ for present conditions, and the initial bed may be considered in transitional regime, between a hydraulically smooth bed and a hydraulically rough bed. In this case, the length scale z_0 may be estimated by (Sleath [43]):

$$z_0 = \frac{k_s}{30}\left[1 - exp\left(-\frac{u'_* k_s}{27v}\right)\right] + \frac{v}{9u'_*} \tag{4}$$

The critical value of the Shields parameter for the sediment incipient motion θ_c is estimated using the relation suggested by Soulsby [44]:

$$\theta_c = \frac{0.3}{1 + 1.2D_*} + 0.055(1 - exp(-0.02D_*)) \tag{5}$$

Fig. 3 Velocity profiles without sediment at x = 6.5 m downstream from the honeycomb. Solid lines represent the best fit for the overlap layer where the velocity profile is logarithmic (least squares method)
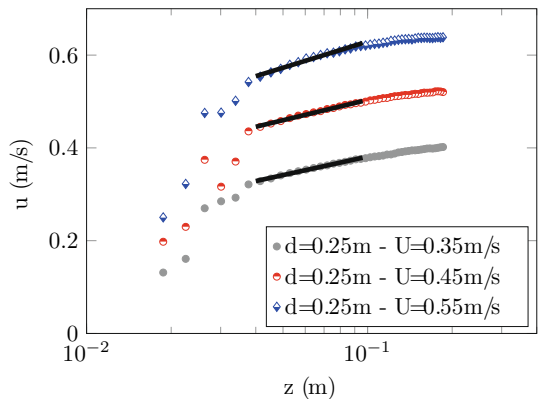
where the dimensionless grain diameter is defined as

$$D_* = \left(\frac{(s-1)g}{v^2} \right)^{1/3} D_{50} \tag{6}$$

The Rouse number,

$$b = \frac{W_s}{\kappa u_*} \tag{7}$$

where W_s is the sediment fall velocity, and u_* the shear velocity at bed estimated with the equilibrium bedforms, is used to define the mode of sediment transport: bedload or suspension. W_s may be estimated using the following equation (Soulsby [44]):

$$W_s = \frac{v}{D_{50}} \left[(10.36^2 + 1.049D_*^3)^{1/2} - 10.36 \right] \tag{8}$$

The roughness length of the bed may be estimated for a bed with ripples or dunes with Eq. 9 which was proposed by van Rijn [51]:

$$k_s = 1.1h_{eq}\left(1 - exp\left(-25\frac{h_{eq}}{\lambda_{eq}} \right) \right) \tag{9}$$

where h_{eq} and λ_{eq} are the bedforms height and length at the equilibrium state, respectively.

The bottom with the bedforms at the equilibrium state is found to be hydraulically rough and z_0 in Eq. 3 can be estimated with (Sleath [43]):

$$z_0 = \frac{k_s}{30} \tag{10}$$

If $b > 2.5$ the bedload transport is dominating and when $b < 2.5$ the sediment transport is dominated by suspension (Bagnold [4]). The sediment transport for all the sets is dominated by bedload ($b > 2.5$; Table 1).

For all the sets, the values of h_{eq} and λ_{eq} were measured.

Finally, the particle Reynolds number, R_{ep}, was used for the estimation of the bedform type (ripple or dune) at the equilibrium state, from the grain size and density (Colombini and Stocchino [16]):

$$R_{ep} = \frac{\sqrt{(s-1)gD_{50}}D_{50}}{v} \tag{11}$$

3 Qualitative observations

Figure 4 illustrates the equilibrium bedforms for sediment supply conditions varying from very limited to unlimited, for the set M2, where ripples can be observed at the equilibrium state. The sediment supply limitation clearly impacts the bed morphology. In particular, an increase of the mean ripple length is observed when the sediment thickness increases.

Three distinct bed states can be identified according to the sediment supply. For very small initial sediment thicknesses (Fig. 4a, b), we observe an alternation of bed structures and large zones uncovered by sand. When the sediment supply increases but

Fig. 4 Top view pictures at the equilibrium state for each initial sediment thickness. Set M2. **a** $\delta = 0.1$ cm, **b** $\delta = 0.5$ cm, **c** $\delta = 1$ cm, **d** $\delta = 2$ cm, **e** $\delta = 3.5$ cm and **f** $\delta = 5.5$ cm. The bottom of the flume appears in black
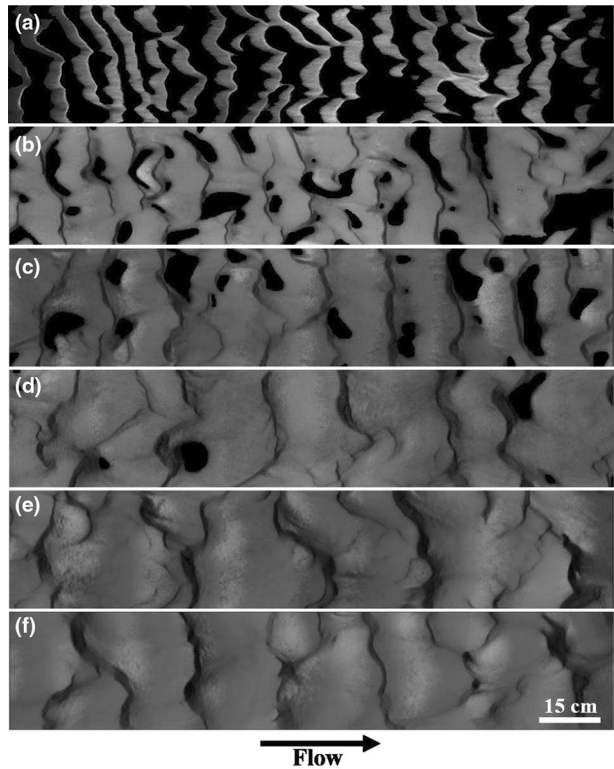
remains limited (Fig. 4c, d), only some patches of uncovered bottom are still visible at the end of the tests. For large sediment supply (Fig. 4e, f), the influence of supply limitation cannot be detected from an observation of the bed surface.

Ripples and dunes in infinite supply conditions are mainly discriminated according to their dimensions, dunes being typically about one order of magnitude higher than ripples and characterized by a length to water depth ratio which is much greater than for ripples (Kennedy [30]; Flemming [25]). It was also reported that no ripples can form for grains of median diameter greater than 0.6 mm (Coleman and Nikora [15]) or 0.8 mm (Soulsby et al. [45]).

The mean wavelengths obtained at the equilibrium state for present tests under limited and unlimited supply conditions are given in Table 2. Due to the irregularity of the equilibrium bedform for set M3, the geometrical parameters could not be estimated accurately. Thus, wavelengths are not included in Table 2 for this set.

In Fig. 5 the present results are shown with the results obtained by Guy et al. [29] from flume experiments under infinite supply conditions. The distinction between ripples and dunes is based on observations and estimations of bedforms dimensions. Ripples are described by Guy et al. [29] as small triangular-shaped bedforms with $\lambda_{eq\_inf} < 0.6$ m and $h_{eq\_inf} < 0.06$ m. Dunes are defined as larger bedforms which do not lead to perturbations of the free surface (Guy et al. [29]). These results which were considered by Colombini and Stocchino [16] are depicted in Fig. 5 where the hydraulic radius R is defined by Eq. 12:

Table 2 Measured mean bedform wavelength at the equilibrium state for each experimental set

	Set M1	Set M2	Set M3	Set C1	Set C2	Set C3
λ_{eq} ($\delta = 0.1$ cm) (m)	0.09	0.09	–	0.51	0.53	–
λ_{eq} ($\delta = 0.5$ cm) (m)	0.09	0.14	–	0.53	0.50	0.85
λ_{eq} ($\delta = 1$ cm) (m)	0.12	0.14	–	0.60	0.45	0.38
λ_{eq} ($\delta = 2$ cm) (m)	0.13	0.18	–	0.86	0.57	0.48
λ_{eq} ($\delta = 3.5$ cm) (m)	0.14	0.20	–	0.57	0.66	0.67
λ_{eq} ($\delta = 5.5$ cm) (m)	0.14	0.18	–	0.68	0.48	0.44
λ_{eq_inf} (m) (present tests)	0.14	0.18	–	0.62	0.53	0.56
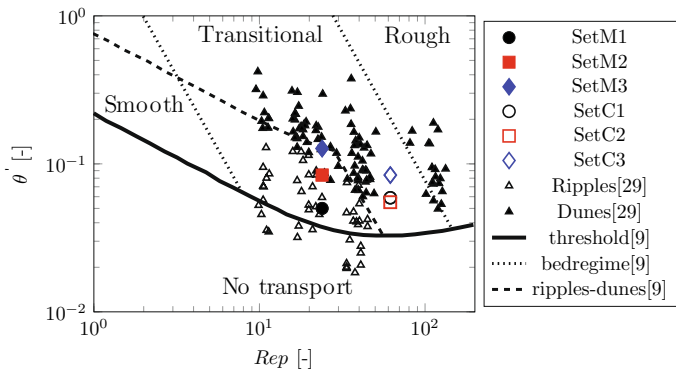
Fig. 5 Effective Shields parameter as a function of the Reynolds number based on the particle diameter. Sets M1 to M3 and C1 to C3: present data. Lines are obtained from Brownlie [9]. From the original representation of Colombini and Stocchino [16]

$$R = \frac{wd}{w + 2d} \qquad (12)$$

with w the flume width.

This figure shows a clear separation between the present sets performed with the medium sand and the sets performed with the coarse one. According to this figure for infinite supply conditions, bedforms for sets M1 and M2 can be considered as ripples and bedforms for sets C1, C2 and C3 as dunes. Set M3 is a set case at the transition from ripples and dunes.

4 Bedload sediment transport

The present paper focuses on bedload transport which is the dominant transport mode for present tests (Sect. 2). To minimize edge effects from the flume configuration, only the sand collected in trap T1 is considered. The dimensionless bedload transport Φ is given by Eq. 13.
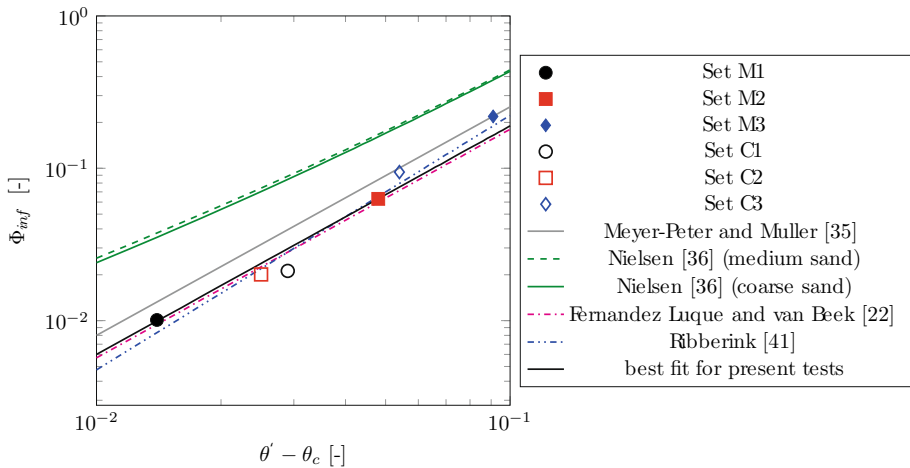
Fig. 6 Sediment bedload transport in infinite sediment supply conditions

Table 3 Parameters used to fit Eq. 15

	n	m	Validity range	Correlation coefficient R^2
Meyer-Peter and Müller [35]	1.5	8	$\theta' < 0.2$	0.89
Fernandez Luque and van Beek [22]	1.5	5.7	$\theta' < 0.1$	0.96
Ribberink [41]	1.67	10.4	$\theta' < 10$	0.96
Present tests	1.5	6	$\theta' < 0.13$	0.97

$$\Phi = \frac{Q_s}{\sqrt{g(s-1)D_{50}^3}} \tag{13}$$

where Q_s is the dimensional bedload transport (m/s^2).

4.1 Unlimited sediment supply conditions

The bedload transport obtained for tests in unlimited supply conditions is compared with formulations from the literature based on the excess of shear stress $\theta' - \theta_c$. The classical formulations of Meyer-Peter and Müller [35], Fernandez Luque and van Beek [22], Nielsen [36] and Ribberink [41] are considered (Fig. 6).

The relation suggested by Nielsen [36] is given by Eq. 14, and the formulation proposed by Meyer-Peter and Müller [35], Fernandez Luque and van Beek [22] and Ribberink [41] is shown in Eq. 15 where Φ_{inf} is the dimensionless bedload transport in infinite sediment supply conditions, and the coefficients m and n are presented in Table 3.

$$\Phi_{inf} = 12\theta'^{\frac{1}{2}}(\theta' - \theta_c) \tag{14}$$

$$\Phi_{inf} = m(\theta' - \theta_c)^n \tag{15}$$

Figure 6 shows that the relation proposed by Nielsen [36] overestimates the bedload transport for the present tests. Based on a conservation equation and an erosion-deposition model, Charru [12] has theoretically shown that Φ_{inf} should be proportional to $\theta'^{3/2}$. Eq. 15 has been fitted to the present data setting the power n to 3/2.

As shown by Wiberg and Smith [53], the parameter m (Eq. 15) can vary from 5 to 15, according to the value of the effective Shields number range. From tests carried out with low values of θ', ($\theta' < 0.1$), Fernandez Luque and van Beek [22] proposed the value 5.7 for the coefficient m, when Meyer-Peter and Müller [35] suggested the value 8 for this coefficient, when $\theta' < 0.2$. For very high values of the effective Shields number ($\theta' > 1$), Nnadi and Wilson [38] proposed m=12. Present values of m and n (Table 3) are very close to the ones obtained by Fernandez Luque and van Beek [22] for coarse sand ($D_{50} > 0.9$ mm), and for the same value range of ($\theta' - \theta_c$) as in present tests. This validates the Fernandez Luque and van Beek [22] formulation for present data. In the following sections, the bedload transport in infinite supply conditions will then be defined according to Eq. 16.

$$\Phi_{inf} = 5.7(\theta' - \theta_c)^{\frac{3}{2}} \tag{16}$$

4.2 Limited sediment supply conditions

Tuijnder [46] and Tuijnder and Ribberink [47] have shown that bedload transport and bedform migration velocity are significantly dependent on the proportion of the bed covered with sediment for limited sediment supply conditions (see Sectd. 4.2 and 5.4). The fraction of the bed covered by sand, $1 - p$ (where p is the uncovered bed fraction) was first introduced by Tuijnder [46]. It was estimated for present tests from top view pictures at the equilibrium state (Fig. 7).

Figure 7 shows that $(1 - p)$ increases for increasing values of the thickness of the sediment layer δ, in agreement with the previous qualitative observations (Sect. 3). For $\delta > 0.03$ m, the bottom is almost fully covered by sediment regardless of the considered sediment size ($D_{50} = 0.328$ mm for sets M, $D_{50} = 0.617$ mm for sets C, and $D_{50} = 0.8$ mm

Fig. 7 Variation of the fraction of the bed covered by sand with the sediment layer thickness from the present tests and the tests of Tuijnder [46]
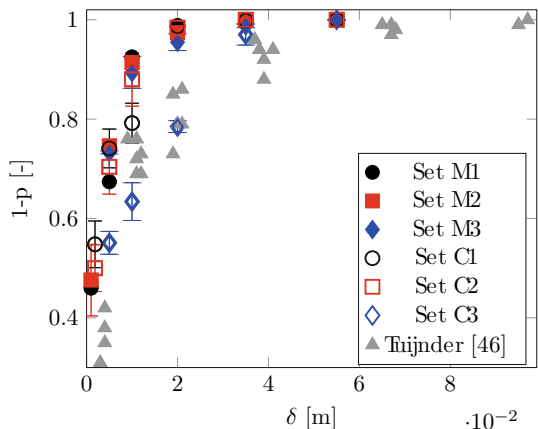
for tests carried out by Tuijnder [46]). Present results show that the bedform type estimated for unlimited supply conditions does not significantly affect the fraction of the bed covered by sand.

For limited sediment supply conditions, zones without mobile sediments do not contribute to the bedload, and the bedload transport is lower than for unlimited sediment supply conditions.

Although Eq. 16 was fitted in a coastal context with a horizontal bed, it can be modified to include the contribution of a sloping bed to the transport in the form:

$$\Phi_{inf} = 5.7\left(\theta' - \theta_c\right)^{\frac{3}{2}} + \Phi_{slope} \tag{17}$$

For Tuijnder experiments conducted in a tiltable flume for alluvial conditions, the Φ_{slope} term was calculated with Eq. 18 derived by Soulsby–van Rijn [44] for rippled beds composed of sand grains ($D_{50} < 2$ mm).

$$\Phi_{slope} = \frac{AU(U - U_c)^{2.4}(-1.6tan(\beta))}{\sqrt{(s - 1)gD_{50}^3}} \tag{18}$$

where

$$A = \frac{0.005d\left(\frac{D_{50}}{d}\right)^{1.2}}{\left((s - 1)gD_{50}\right)^{1.2}} \tag{19}$$

and U_c is the threshold mean current velocity estimated from Eqs. 2, 3 and 5.

The flume slope β was set equal to the average slope of energy level I_e since uniform flow condition was verified in the set of Tuijnder tests used (Tuijnder [46]).

For supply limited conditions, Eq. 20 can be used to compare with present data calculating Φ_{inf} with Eqs. 17–19.

$$\Phi = (1 - p)\,\Phi_{inf} \tag{20}$$

Figure 8 shows a comparison of present data fitted with Eq. 20 and data from Tuijnder [46]. It can be seen that a very good agreement is found ($R^2 = 0.92$).

The bedload transport in sediment supply limited conditions may then be obtained only from the fraction of the bed covered by sand, the critical value of the Shields parameter for initial motion, and the effective Shields parameter.

5 Bedforms migration velocity

5.1 Qualitative results from present tests

The spatio-temporal images obtained from video acquisitions (top views, see Sect. 2) allow to estimate the bedforms migration velocities. Figure 9 shows spatio-temporal diagrams for the Set M2, where the bedforms crests may be easily identified. The inclination of the crests indicates the mean migration velocity of the bedforms.

In Fig. 9 the thickness δ of the initial sediment layer varies between 0.1 cm (Fig. 9a) and 5.5 cm (Fig. 9f). It can be deduced from this figure that the mean migration velocity is

Fig. 8 Bedload transport in sand supply limited conditions. Comparison between measurements from the present tests and data from Tuijnder [46] and calculations from Eq. 20. Solid line: perfect agreement between measured and predicted (Eq. 20) bedload transport; dashed lines: 5% difference between measured and predicted (Eq. 20) bedload transport
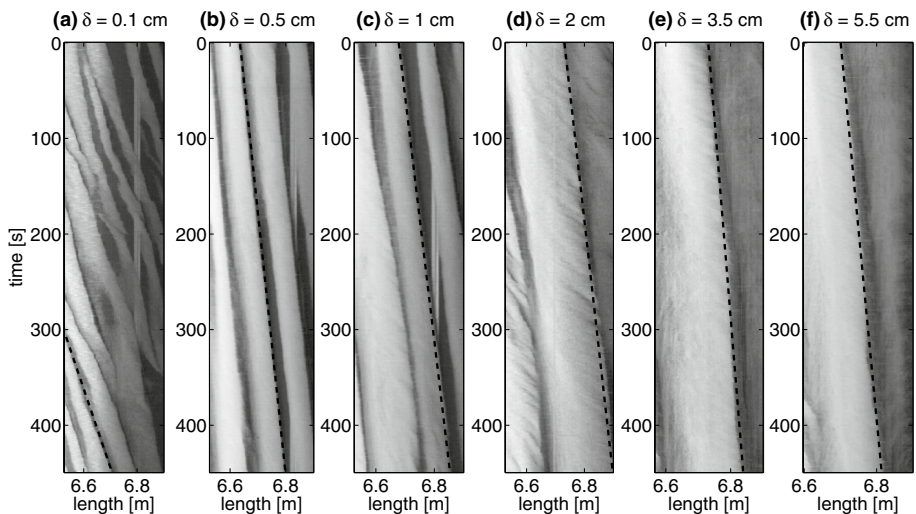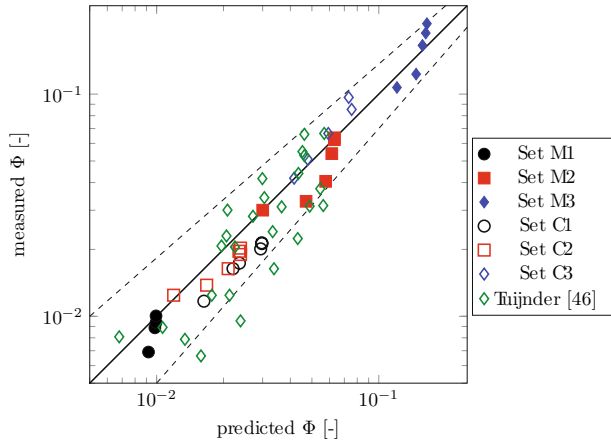
Fig. 9 Spatio-temporal diagrams at the equilibrium state, for different thicknesses of the initial sediment layer, for Set M2. The dashed lines exhibit indicative bedforms crest positions. The flow is from left to right

higher for strong supply limited conditions when uncovered regions are extended than for unlimited supply conditions. This is observed for all sets of present tests, in agreement with Tuijnder [46]. This is due to the smaller dimensions of bedforms under limited supply conditions for identical hydrodynamic conditions. As mentioned by Bagnold [3], the decrease of the migration velocity for increasing values of bedform heights can be explained from mass conservation.

5.2 Re-analysis of data from Ferret [23]

These data have been acquired on a dune field in the Eastern English Channel, off Dieppe (France), where macrotidal conditions (8.5 m tidal range in mean spring

conditions) prevail and where the water depth varies from 11 to 23 m (Fig. 10). The dune characteristics have been measured during the summers 2007 and 2008. A multi-beam echosounder (EM1000 95 kHz KONGSBERG) was used for the bathymetry, an acoustic Doppler current profiler (ADP Sontek 1 MHz and ADCP RDI 1.2 MHz) for the current velocities, and a side-scan sonar (EDGETECH DF 1000 DCI) for the sediment distribution on the sea bed. Surficial sediment samples were collected for the calibration of the side-scan sonar (data location on Fig. 10).

Two zones can be identified on the dune field: one in the western part where the sediment supply is limited and one in the central and eastern parts where the sediment supply is unlimited (Fig. 10). From west to east, a morpho-sedimentary gradient is observed as a consequence of the speed decrease of tidal currents (Table 4). In the western part, under supply limitation, dunes heights and wavelengths are respectively in the range 3.4–8.5 m and 100–920 m with barchanoid asymmetrical shapes (very large dunes, named VL dunes following Ashley [2]). The bedforms are composed of gravelly sand with an approximately 1.03 mm median diameter D_{50}, and lie on a coarser seabed made of sandy gravel (Fig. 10). In the central and eastern parts, under unlimited supply conditions, dunes are more rectilinear, with smaller heights in the range 1.15–3.6 m and wavelengths between 220 and 940 m (large dunes, named L dunes). Numerous medium to large dunes (named ML dunes) are also observed in these parts with heights of several decimetres and wavelengths between 10 and 35 m. They are composed of sediments varying from gravelly sand to sand, with a median diameter D_{50} in the range 0.23–0.92 mm.

A bathymetric reference profile has been measured several times in 2007 and 2008, in fair weather conditions, allowing to measure the dune migration under tidal forcing at various short time steps and for limited and unlimited sediment supply conditions (Table 5). Geographic Information System tools (ArcGIS® ESRI) have allowed: (i) to measure the dune migration for different times, from Digital Elevation Models,
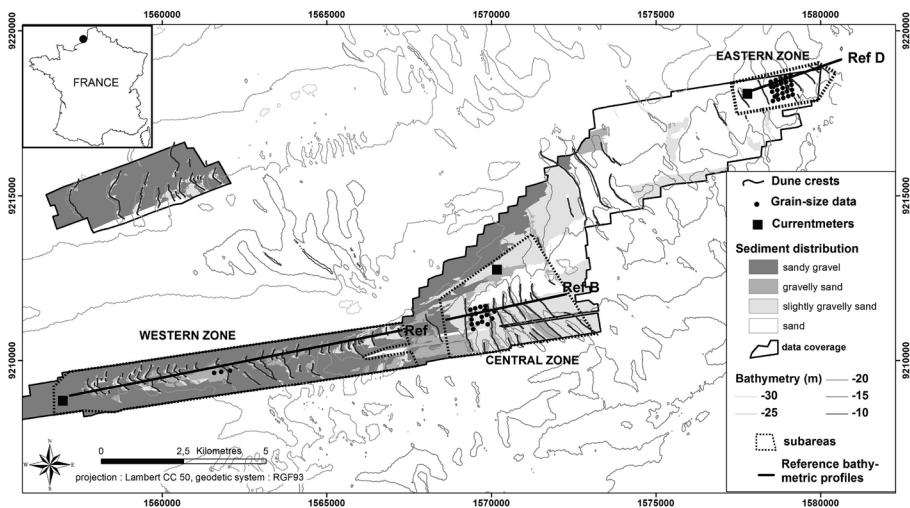
Fig. 10 Dune field in the Eastern English Channel in limited (western zone) and unlimited (central and eastern zones) sediment supply conditions. Field data from Ferret [23]. General bathymetry from Shom (Service hydrographique et océanographique de la Marine—France)

Table 4 Morpho-sedimentary characteristics of the different zones

Zone	Bedform heights (m)	Bedform wavelengths (m)	D_{50} (mm)	σ_g^2 (–) (Soulsby [44])	Sediment type (Folk [27])
Western zone	6.5 (3.4–8.5)	530 (100–920)	1.03 (0.9–1.23)	3.90 (3.58–3.97)	Gravelly sands (73–77% sands)
Central zone	3.0 (2.5–3.6)	430 (305–940)	0.55 (0.34–0.92)	3.78 (2.40–4.79)	Gravelly sands (70–88% sands)
Eastern zone	2.2 (1.15–2.85)	440 (220–700)	0.27 (0.23–0.31)	1.59 (1.48–1.61)	Sands

Table 5 Sediment and bedforms characteristics for Ferret [23] field data, and observation times

Sediment supply	Fraction of the bed covered by sand	Area considered in the observation field	Reference profiles for the estimation of the migration velocity	Observation time	Bedform type
Limited	0.33	Western	Ref	Flood (spring)	Barchanoid VL dunes
Limited	0.33	Western	Ref	2 days (neap)	Barchanoid VL dunes
Limited	0.33	Western	Ref	2 days (spring)	Barchanoid VL dunes
Limited	0.33	Western	Ref	12 days	Barchanoid VL dunes
Unlimited	1	Central	RefB	Flood (spring)	L dunes
Unlimited	1	Central	RefB	1 day (spring)	L dunes
Unlimited	1	Central	RefB	1 day (spring)	L dunes
Unlimited	1	Eastern	RefB	2 days (neap)	L dunes + ML dunes
Unlimited	1	Central	RefB	6 days	L dunes
Unlimited	1	Eastern	RefD	12 h (spring)	L dunes
Unlimited	1	Eastern	RefD	1 day (neap)	L dunes

The profiles "Ref", "RefB", "RefD" are respectively in the western, central and eastern areas (Fig. 10). VL, L and ML dunes referred to very large, large and medium dunes

obtained by interpolation of bathymetric data, and (ii) to calculate the covered bed fraction $(1 - p)$ from sediment distribution data.

5.3 Unlimited sediment supply conditions

Florez and Franklin [26] found two different behaviours for the dimensionless bedform migration velocity under unlimited supply conditions, c_{inf}/u'_*, where c_{inf} is the mean migration velocity under unlimited supply conditions, according to the value of $(\theta' - \theta_c)$. Based on experiments in a closed flume conducted with glass beads, they found a threshold for $(\theta' - \theta_c) = 3.10^{-2}$. The type of bedforms observed during their experiments is not specified. Below the threshold, they found that the dimensionless migration velocity is proportional to $(\theta' - \theta_c)^{3/2}$ in accordance with Meyer-Peter and Müller [35] transport rate equation. Above the threshold, they found that c_{inf}/u'_* is proportional to $(\theta' - \theta_c)^{5/2}$.

Figure 11 depicts the variation of the dimensionless bedform migration velocity c_{inf}/u'_* with the dimensionless shear stress excess $(\theta' - \theta_c)$ for present tests and for the results in the Eastern English Channel issued from Ferret [23] data. The results obtained by Florez and Franklin [26] in a closed flume with glass beads, by Tuijnder [46] in a fluvial flume with natural sand, by Durafour [19] in the field in Eastern English Channel, by Doré [17] in the bay of Arcachon, and by Claude et al. [14] and Wintenberger et al. [54] in the Loire river, are also depicted in Fig. 11. The main characteristics of these data are given in Table 6.

Figure 11 shows that for the data considered in this figure, the threshold value for $(\theta' - \theta_c)$ is approximately 0.1. The sudden decrease in the bedform migration velocity at this threshold is probably due to the increasing part of the suspension transport that is not efficient for migration. It can be noticed that the values of the Rouse number (see Table 6) for the data which are below this threshold in Fig. 11 are greater than $\simeq 2.5$, which corresponds to a sediment transport dominated by bedload (Sect. 2), and the values of the Rouse number are smaller than $\simeq 2.5$ for the data above this threshold, for which the transport by suspension is dominant. This is clearly illustrated in Fig. 12. The dominant mode for sediment transport can be bedload at a given time for a bedform field, when suspensions can become dominant for this field, following an increase in the mean flow velocity. This was the case for Ferret [23] and Doré [17] measurements in the field, and data from these authors appear for $(\theta' - \theta_c) < 0.1$ and for $(\theta' - \theta_c) > 0.1$ in Fig. 11.

For $(\theta' - \theta_c) < 0.1$, the bedforms migration velocity is proportional to $(\theta' - \theta_c)^{3/2}$ for natural sands [17, 19, 23, 48] as for glass beads [26]. However the migration velocity is lower for natural sands due to the influence of the sediment grain shape. This is not surprising since it is well known that the particle shape is a significant parameter for the hydrodynamic behaviour of grains (Lane and Carlson [32], Durafour et al. [20]). Field measurements in tidal environment for small observation time intervals [17, 19] or quite large time intervals (a few days, [23]) are in good agreement with the present flume data.

For $(\theta' - \theta_c) > 0.1$, the bedforms migration velocities are close for field measurements in the Loire [14, 54] where the bed is composed of coarse ($D_{50} \simeq 1$ mm) and slightly heterogeneous sediments, in the Arcachon bay [17] with medium ($D_{50} = 0.32$ mm) size well-sorted sediments, and in the Eastern English Channel with large dunes and heterogeneous sediments. In other words, no clear dependence of the dimensionless migration velocity with $\theta' - \theta_c$ is observed when $(\theta' - \theta_c) > 0.1$.

The migration velocity does not depend on the type of bedforms (ripples or dunes) for a fixed value of $\theta' - \theta_c$. This figure also shows that the dimensionless bedforms migration

Table 6 Characteristics for unlimited sediment supply conditions of the experimental and field data used in Fig. 11

	Conditions	Sediment type	Slope (–)	Bedform types	h_{eq} (m)	b (–)
Set M1	Flume	Natural sand	–	Ripples	0.013	10
Set M2	Flume	Natural sand	–	Ripples	0.016	7.5
Set M3	Flume	Natural sand	–	–	–	–
Set C1	Flume	Natural sand	–	Dunes	0.013	8.6
Set C2	Flume	Natural sand	–	Dunes	0.01	9.3
Set C3	Flume	Natural sand	–	Dunes	0.019	6.5
Ferret [23]	Coastal (Eastern English Channel)	Natural sand	–	L dunes	1.15–3.6	1.1–4.5
Ferret [23]	Coastal (Eastern English Channel)	Natural sand	–	ML dunes	0.5	7.6
Tuijnder [46]	Flume	Natural sand	0.0007–0.0022	Dunes	0.067–0.091	4.2–5.1
Florez and Franklin [26]	Closed flume	Glass bead	–	Unspecified	–	–
Durafour [19]	Coastal (Eastern English Channel)	Natural sand	–	Ripples	$\simeq 0.05$	4.4
Wintenberger et al. [54]	River (Loire)	Natural sand	0.0003	Dunes	0.1–0.3	1.9–3.1
Claude et al. [14]	River (Loire)	Natural sand	0.0003	Dunes	0.1–0.3	3.2–3.4
Doré [17] (dunes)	Coastal (Bay of Arcachon)	Natural sand	–	Dunes	$\simeq 2$	1.7–2.7
Doré [17] (superimposed ripples)	Coastal (Bay of Arcachon)	Natural sand	–	Ripples	$\simeq 0.2$	1.9–2.3

Fig. 11 Variation of the dimensionless bedform migration velocity c_{inf}/u'_* with $(\theta' - \theta_c)$ for unlimited sediment supply conditions
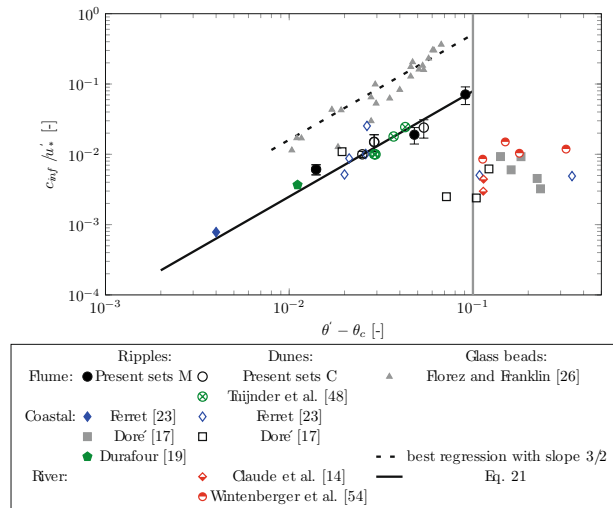
**Fig. 12** Rouse number as a function of $(\theta' - \theta_c)$. Symbols are defined in Fig. 11
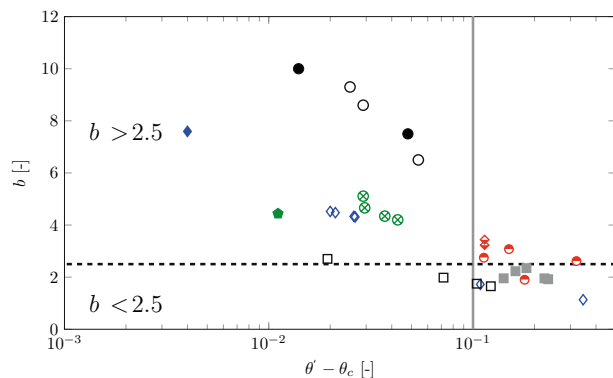
velocity can be estimated under unlimited sediment supply conditions for natural sediments by the following equation, when $\theta' - \theta_c < 0.1$ ($R^2 = 0.93$), inducing values of the Rouse number greater than 2.5 and sediment transport dominated by bedload:

$$\frac{c_{inf}}{u'_*} = 2.5(\theta' - \theta_c)^{3/2} \tag{21}$$

5.4 Limited sediment supply conditions

It has been mentioned in Sect. 5.1 that the bedforms migration velocity is higher under limited sediment supply conditions, when bed regions are uncovered by sediments, than for unlimited sediment supply conditions. Figure 13 depicts the variation of the dimensionless bedform migration velocity c/u'_*, where c is the mean migration velocity, with $(\theta' - \theta_c)/(1 - p)$. This figure shows that an adaptation of the formulation proposed for the dimensionless bedforms migration velocity in unlimited supply conditions (Eq. 21) may

Fig. 13 Variation of the dimensionless bedform migration velocity c/u'_* with $(\theta' - \theta_c)/(1 - p)$ for limited sediment supply conditions
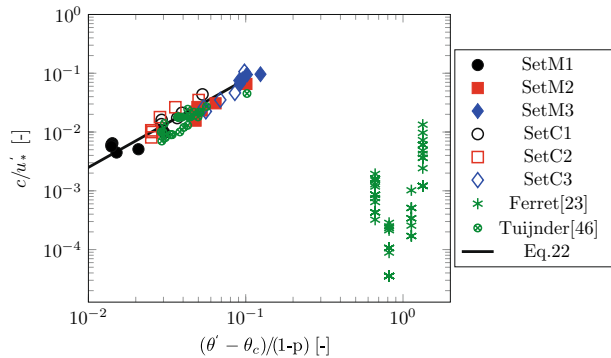
satisfactorily describe the results obtained by Tuijnder [46] and present tests under limited supply conditions when $\theta' - \theta_c < 0.1$. This adaptation, based on the fraction of the bed covered by sand $(1 - p)$, is given by Eq. 22 ($R^2 = 0.86$) (Fig. 13).

$$\frac{c}{u'_*} = \frac{2.5}{1 - p}(\theta' - \theta_c)^{3/2} \tag{22}$$

For $(\theta' - \theta_c) > 0.1$, the results depicted in Fig. 13 obtained from field data in the Eastern English Channel (Ferret [23]) are very scattered, and may be affected by the modification of sediment transport mode with a transport dominated by suspension.

6 Conclusions

Tests have been carried out in a flume with medium and coarse sand to study the effect of sediment supply limitation on bedload transport and bedforms migration velocity. Field data obtained in the Eastern English Channel in limited and unlimited sediment supply conditions by Ferret [23] have also been analyzed.

Present results show that the formulation proposed by Fernandez Luque and van Beek [22] (Eq. 16) for coarse sand bedload transport in unlimited sediment supply conditions is suitable for medium and coarse sand, when the effective Shields parameters θ' is such as $(\theta' - \theta_c) < 0.1$, where θ_c is the critical value of the Shields parameter for the sediment initial motion. In the case of limited sediment supply conditions, the fraction of the bed covered by sediments $(1 - p)$ mainly depends on the initial thickness of the sediment layer. The bedload transport for limited sediment supply conditions is found to be proportional to $(1 - p)$ (Eq. 20).

Concerning the dimensionless migration velocity, two different behaviours are found depending on whether the excess of shear stress $(\theta' - \theta_c)$ is below or above the threshold value 0.1. This is explained by a change of the sediment transport mode from bedload dominated when $(\theta' - \theta_c) < 0.1$ to suspension dominated when $(\theta' - \theta_c) > 0.1$. A new expression (Eq. 21) exhibiting a good agreement with flume and field data is proposed for the dimensionless ripples and dunes migration velocity under unlimited sediment supply conditions when the sediment transport is dominated by bedload. An adaptation of this formulation (Eq. 22), based on the fraction of the bed covered by sand, is proposed for the dimensionless velocity of bedforms under limited sediment supply conditions when

bedload is the dominant mode of sediment transport. This adaptation is obtained from flume data sets.

References

1. Allen J (1968) The nature and origin of bed-form hierarchies. Sedimentology 10(3):161–182
2. Ashley GM (1990) Classification of large-scale subaqueous bedforms; a new look at an old problem. J Sediment Res 60(1):160–172
3. Bagnold RA (1941) The physics of blown sand and desert dunes. Methuen, London
4. Bagnold RA (1966) An approach to the sediment transport problem from general physics. US government printing office
5. Belderson R, Johnson MA, Kenyon NH (1982) Bedforms. Offshore tidal sands: processes and deposits. Chapman and Hall, London
6. Berni C, Perret E, Camenen B (2018) Characteristic time of sediment transport decrease in static armour formation. Geomorphology 317:1–9
7. Blondeaux P (2001) Mechanics of coastal forms. Annu Rev Fluid Mech 33(1):339–370
8. Blondeaux P, Vittori G, Mazzuoli M (2016) Pattern formation in a thin layer of sediment. Mar Geol 376:39–50
9. Brownlie WR (1981) Prediction of flow depth and sediment discharge in open channels. Technical Report KH-R-43A California Institute of Technology, Pasadena, CA
10. Carling P, Golz E, Orr H, Radecki-Pawlik A (2000) The morphodynamics of fluvial sand dunes in the River Rhine, near Mainz, Germany. I. Sedimentology and morphology. Sedimentology 47(1):227–252
11. Carling P, Williams J, Golz E, Kelsey A (2000) The morphodynamics of fluvial sand dunes in the River Rhine, near Mainz, Germany. II. Hydrodynamics and sediment transport. Sedimentology 47(1):253
12. Charru F (2006) Selection of the ripple length on a granular bed sheared by a liquid flow. Phys Fluids 18(12):121508
13. Charru F, Andreotti B, Claudin P (2013) Sand ripples and dunes. Annu Rev Fluid Mech 45:469–493
14. Claude N, Rodrigues S, Bustillo V, Bréhéret JG, Macaire JJ, Jugé P (2012) Estimating bedload transport in a large sand-gravel bed river from direct sampling, dune tracking and empirical formulas. Geomorphology 179:40–57
15. Coleman S, Nikora V (2011) Fluvial dunes: initiation, characterization, flow structure. Earth Surf Proc Land 36(1):39–57
16. Colombini M, Stocchino A (2011) Ripple and dune formation in rivers. J Fluid Mech 673:121–131
17. Doré A (2015) Modélisation de l'évolution morphodynamique des dunes sous-marines. Ph.D. thesis, Université de Bordeaux, France
18. Dreano J, Valance A, Lague D, Cassar C (2010) Experimental study on transient and steady-state dynamics of bedforms in supply limited configuration. Earth Surf Proc Land 35(14):1730–1743
19. Durafour M (2014) Dynamique sédimentaire en zone côtière dans le cas de sédiments hétérogènes: application au domaine côtier haut-normand. Ph.D. thesis, Université du Havre, France, 260 pp
20. Durafour M, Jarno A, Le Bot S, Lafite R, Marin F (2015) Bedload transport for heterogeneous sediments. Environ Fluid Mech 15(4):731–751
21. Engelund F, Fredsoe J (1982) Sediment ripples and dunes. Annu Rev Fluid Mech 14(1):13–37
22. Fernandez Luque R, Van Beek R (1976) Erosion and transport of bed-load sediment. J Hydraul Res 14(2):127–144
23. Ferret Y (2011) Morphodynamique des dunes sous-marines en contexte de plate-forme mégatidale (manche orientale). approche multi-échelles spatio-temporelles. Ph.D. thesis, Université de Rouen, France, 305 pp
24. Ferret Y, Le Bot S, Tessier B, Garlan T, Lafite R (2010) Migration and internal architecture of marine dunes in the Eastern English channel over 14 and 56 year intervals: the influence of tides and decennial storms. Earth Surf Proc Land 35(12):1480–1493
25. Flemming B (2000) A revised textural classification of gravel-free muddy sediments on the basis of ternary diagrams. Cont Shelf Res 20(10–11):1125–1137
26. Florez JEC, Franklin EM (2016) The formation and migration of sand ripples in closed conduits: experiments with turbulent water flows. Exp Thermal Fluid Sci 71:95–102
27. Folk RL (1954) The distinction between grain size and mineral composition in sedimentary-rock nomenclature. J Geol 62(4):344–359

28. Franklin EM, Charru F (2011) Subaqueous barchan dunes in turbulent shear flow. Part 1. Dune motion. J Fluid Mech 675:199–222
29. Guy HP, Simons DB, Richardson EV (1966) Summary of alluvial channel data from flume experiments, 1956–1961. US Government Printing Office
30. Kennedy JF (1963) The mechanics of dunes and antidunes in erodible-bed channels. J Fluid Mech 16(4):521–544
31. Kleinhans MG, van Rijn LC (2002) Stochastic prediction of sediment transport in sand-gravel bed rivers. J Hydraul Eng 128(4):412–425
32. Lane E, Carlson E (1954) Some observations on the effect of particle shape on the movement of coarse sediments. Eos Trans Am Geophys Union 35(3):453–462
33. Le Bot S, Trentesaux A (2004) Types of internal structure and external morphology of submarine dunes under the influence of tide-and wind-driven processes (Dover Strait, northern France). Mar Geol 211(1–2):143–168
34. Mazzuoli M, Kidanemariam AG, Blondeaux P, Vittori G, Uhlmann M (2016) On the formation of sediment chains in an oscillatory boundary layer. J Fluid Mech 789:461–480
35. Meyer-Peter E, Müller R (1948) Formulas for bed-load transport. In: IAHSR 2nd meeting, Stockholm, Appendix 2, IAHR
36. Nielsen P (1992) Coastal bottom boundary layers and sediment transport, vol 4. Advanced series on ocean engineering. World Scientific Publishing Company, Singpore
37. Nielsen P (2009) Coastal and estuarine processes, vol 29. Advanced series on ocean engineering. World Scientific Publishing Company, Singapore
38. Nnadi FN, Wilson KC (1992) Motion of contact-load particles at high shear stress. J Hydraul Eng 118(12):1670–1684
39. Porcile G, Blondeaux P, Vittori G (2017) On the formation of periodic sandy mounds. Cont Shelf Res 145:68–79
40. Rauen WB, Lin B, Falconer RA (2009) Modelling ripple development under non-uniform flow and sediment supply-limited conditions in a laboratory flume. Estuar Coast Shelf Sci 82(3):452–460
41. Ribberink JS (1998) Bed-load transport for steady flows and unsteady oscillatory flows. Coast Eng 34(1–2):59–82
42. Seminara G (2010) Fluvial sedimentary patterns. Annu Rev Fluid Mech 42:43–66
43. Sleath JF (1984) Sea bed mechanics. Wiley, New York, NY
44. Soulsby R (1997) Dynamics of marine sands: a manual for practical applications. Thomas Telford
45. Soulsby RL, Whitehouse RJS, Marten KV (2012) Prediction of time-evolving sand ripples in shelf seas. Cont Shelf Res 38:47–62
46. Tuijnder A (2010) Sand in short supply: modelling of bedforms, roughness and sediment transport in rivers under supply-limited conditions. Ph.D. thesis, University of Twente, Nederlands
47. Tuijnder AP, Ribberink JS (2012) Experimental observation and modelling of roughness variation due to supply-limited sediment transport in uni-directional flow. J Hydraul Res 50(5):506–520
48. Tuijnder AP, Ribberink JS, Hulscher SJ (2009) An experimental study into the geometry of supply-limited dunes. Sedimentology 56(6):1713–1727
49. Vah M, Jarno A, Le Bot S, Marin F (2018) Experimental study on sediment supply-limited bedforms in a coastal context. In: Proceedings, 6th International Conference on Estuaries and Coasts, ICEC2018, Caen, France
50. Van Landeghem KJ, Uehara K, Wheeler AJ, Mitchell NC, Scourse JD (2009) Post-glacial sediment dynamics in the Irish sea and sediment wave morphology: data-model comparisons. Cont Shelf Res 29(14):1723–1736
51. Van Rijn LC (1982) Equivalent roughness of alluvial bed. J Hydraul Div 108(10):1215–1218
52. Wentworth CK (1922) A scale of grade and class terms for clastic sediments. J Geol 30(5):377–392
53. Wiberg PL, Dungan Smith J (1989) Model for calculating bed load transport of sediment. J Hydraul Eng 115(1):101–123
54. Wintenberger CL, Rodrigues S, Claude N, Jugé P, Bréhéret JG, Villar M (2015) Dynamics of nonmigrating mid-channel bar and superimposed dunes in a sandy-gravelly river (Loire River, France). Geomorphology 248:185–204